Table II. Radial Distribution of Atoms about Mn and Mn–O–P Angles in $H_2MnP_3O_{10}\cdot 2H_2O$

atom type	coordn no.	radial dist, Å	Debye–Waller factor ($2\sigma^2$), Å^2
O(1)	4	1.86	0.007
O(2)	1	2.24	0.007
O(3)	1	2.09	0.007
P(1)	4	3.14	0.008
P(2)	1	3.37	0.008
P(3)	1	3.27	0.008

Mn–O–P	angle, deg
Mn–O(1)–P(1)	135
Mn–O(2)–P(2)	125
Mn–O(3)–P(3)	130

manganese in $MnPO_4\cdot H_2O$.[6] The octahedral coordination of oxygens is distorted axially, because both compounds show a Jahn–Teller effect, although in the second compound it is larger.

Values of Mn–O distances and Debye–Waller factors were refined to obtain the best fit between theory and experiment. Then, calculations were performed for phosphorus in the second shell and for multiple scattering within the three-atom array Mn–O–P to obtain the refined Mn–O–P angles.

Refinement of the radial distances (Mn–O and Mn···P), Debye–Waller factors, and the Mn–O–P angles led to a very satisfactory level of agreement between the observed and calculated spectra and its Fourier transform, as illustrated in Figure 4. The values of the refined parameters are listed in Table II.

The Mn–O–P framework consists of axially distorted MnO_6 octahedra that share all six corners with PO_4 tetrahedra. The observed bond distances 4 × 1.86, 1 × 2.09, and 1 × 2.24 Å are similar to those in other manganese(III) oxide systems: Mn_2O_3,[29] which has 4 × 1.90 and 2 × 2.24 Å; $NaMnO_2$,[30] with 4 × 1.92 and 2 × 2.40 Å; $MnPO_4\cdot H_2O$,[6] having 2 × 1.89, 2 × 1.91, and 2 × 2.28 Å; and $Mn(PO_3)_3$,[5] with 2 × 1.88, 2 × 1.91, and 2 × 2.16 Å.

The P–O distances may be calculated from the Mn–O and Mn–P distances and the angles obtained from multiple-scattering calculations. The manganese(III) environment with all distances (Å) and angles (deg) obtained from the EXAFS study is shown in I.

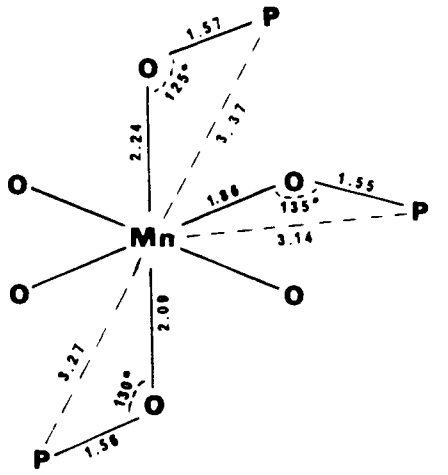

I

The manganese(III) environment confirms the Jahn–Teller effect that is seen in the diffuse-reflectance spectrum. This environment is less distorted than that observed in manganese(III) orthophosphate hydrate,[6] in agreement with the diffuse-reflectance results.[3]

The layered framework of this compound has been proved from a butylamine intercalation experiment in the vapor phase. The basal spacing increases from 7.77 to 15.45 Å after *n*-butylamine intercalation. However, only the first reflection line is sharp and the X-ray powder pattern at high angles (2θ) is poor.

Acknowledgment. We acknowledge helpful discussions with Dr. J. P. Attfield (University of Oxford, U.K.) and Dr. J. Garcia-Ruiz (Universidad de Zaragoza, Spain) and thank the Comisiôn Interministerial de Ciencia y Tecnologia (CICYT, Spain) and Istituto Nazionale di Fisica Nucleare (INFN, Italy) for use of the facility at Frascati. M.A.G.A. and J.C. also wish to thank the Ministerio de Educación y Ciencia (Spain) for the provision of studentships.

(29) Geller, S. *Acta Crystallogr.* **1971**, *B27*, 821.
(30) Jansen, M.; Hoppe, R. *Z. Anorg. Allg. Chem.* **1973**, *399*, 163.

Contribution from the Department of Chemistry, University of South Carolina, Columbia, South Carolina 29208

Luminescence Studies of Tris[dihydrobis(1-pyrazolyl)borato]terbium(III)

Daniel L. Reger,* Pi-Tai Chou,* Shannon L. Studer, Steven J. Knox, Marty L. Martinez, and William E. Brewer

Received April 27, 1990

The luminescence spectra and dynamics of $[H_2B(pz)_2]_3Tb$ have been studied at different temperatures, in the solid phase and in various solvents. Analysis of the data for the crystalline sample based on the electron dipole selection rules reveals effective C_3 symmetry about the terbium atom. Thus, the luminescence spectra are those expected for the trigonal-prismatic arrangement of the nitrogen donor atoms but influenced by the three weak BH···Tb three-center bonds to each of the rectangular faces. Similar luminescence spectra are observed for $[H_2B(pz)_2]_3Tb$ in CH_2Cl_2 and toluene solutions. In donor solvents, complexation of $[H_2B(pz)_2]_3Tb$ with the solvent molecules changes the lifetime and the spectral feature of the luminescence, indicating a change in the coordination environment about the terbium atom.

Introduction

We have recently been exploring the chemistry of early metals and the lanthanides using the versatile poly(pyrazolyl)borate ligand system.[1] A particularly interesting complex that we have prepared and carefully characterized by multinuclear NMR and single crystal X-ray crystallography is $[H_2B(pz)_2]_3Y$ (**1**, pz = pyrazolyl ring).[1a] In the solid state, the six nitrogen donor atoms of the bis(pyrazolyl)borate ligands are arranged in a trigonal-prismatic array. In addition, the six-membered YN_4B rings are oriented in a puckered boat configuration that brings one of the hydrogen atoms on each of the three boron atoms in close proximity to the yttrium metal, indicating the formation of three three-center, two-electron BH···Y bonding interactions (agostic bonds). A

(1) (a) Reger, D. L.; Lindeman, J. A.; Lebioda, L. *Inorg. Chem.* **1988**, *27*, 1890. (b) Reger, D. L.; Lindeman, J. A.; Lebioda, L. *Ibid.* **1988**, *27*, 3923. (c) Reger, D. L.; Knox, S. L.; Lindeman, J. A.; Lebioda, L. *Ibid.* **1990**, *29*, 416.

0020-1669/91/1330-2397$02.50/0

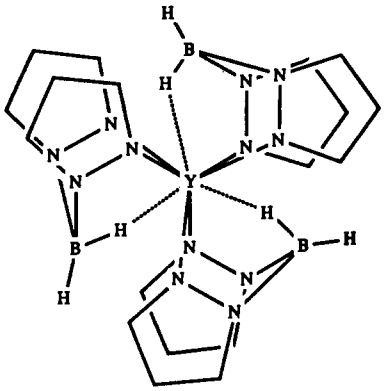

1

number of examples of molecules containing one BH---M three-center bond have been reported previously.[2-4] In all of these studies, the agostic interaction in the solid state was confirmed crystallographically. In addition, in two cases, the interaction was confirmed in solution from the difference in the boron–hydrogen coupling constants between the terminal (J_{BH} = 118 Hz) and bridging (J_{BH} = 76–88 Hz) BH_2 hydrogen atoms.[4] This technique was not definitive for **1** in solution (fluxional processes equilibrate the BH_2 hydrogen atoms), but other studies, primarily the variable-temperature ^2H NMR spectra of $[D_2B(pz)_2]_3Y$, did demonstrate that the agostic interactions were still present in CH_2Cl_2 solution.[1a]

We have expanded this chemistry of yttrium to three representative lanthanide metals, samarium, terbium, and erbium, and have prepared the analogous $[H_2B(pz)_2]_3M$ complex for each.[1c] With these paramagnetic metals, meaningful NMR spectra could only be obtained for the samarium complex. From the similarity of the variable-temperature NMR data for the yttrium and samarium complexes and of the infrared data for all four, we concluded that these lanthanide complexes all had the same unusual structure as **1**. The similarity in structure is especially expected for $[H_2B(pz)_2]_3Tb$ (**2**), the molecule of interest here, because yttrium(III) and terbium(III) are essentially the same size.[5]

Reported here is a detailed study of the luminescence of $[H_2B(pz)_2]_3Tb$ both in the solid state and dissolved in a variety of solvents. This study is of interest because of the unusual trigonal-prismatic arrangement of the nitrogen donor atoms about $[H_2B(pz)_2]_3Tb$ and our desire to determine if the weak three-center interactions would have a measurable impact on the solid-phase spectra. We also wished to determine how solvent interactions would change the coordination environment for $[H_2B(pz)_2]_3Tb$ in solution. The luminescence spectra of several other Tb(III) complexes with a variety of coordination environments in solid and solution phases have been reported by Brittain et al.[6-8]

Experimental Section

Sample Preparation. All operations were carried out under a nitrogen atmosphere either by standard Schlenk techniques or in a Vacuum Atmospheres HE-493 drybox. All solvents were dried, degassed, and distilled prior to use. $[H_2B(pz)_2]_3Tb$ was prepared by the published method.[1c] The solid samples were prepared by loading $[H_2B(pz)_2]_3Tb$ into a Pyrex capillary in the drybox, transporting the sample under nitrogen to a vacuum line, and sealing the capillary. The solution samples were prepared by dissolving $[H_2B(pz)_2]_3Tb$ in the appropriate solvent, following the same procedure; however, the bottom of the capillary was immersed in liquid nitrogen before being evacuated and sealed on the vacuum line.

Measurements. The third harmonic (355 nm, 8 ns) of a Nd:YAG laser (Quantel Model 580) was used as the excitation pulse. Occasionally, the $^7F_6 \rightarrow {}^5D_4$ excitation is achieved by a tunable flash-lamp-pumped dye laser (Phase-R Model 120V) at 480–484 nm (vide infra). The sample, situated in a cryostat (Model DTC-500 Lake Shore Cryotronics, Inc.), was excited by the laser pulse and the emission collected at 90°. Measurements at 77 K were performed by using a quartz liquid-nitrogen dewar. The detection system consists of an optical multichannel analyzer (OMA) system, which couples with a gateable intensified silicon photodiode array (EG&G/PAR, Model 1420) and a 0.5-m monochromator (Spex Model 1870). The emission was focused to the slit of the monochromator by a 5 cm focal length quartz lens. With the slit width open to 30 μm and a 1200 grooves/mm grating, a resolution of 1.5 Å was determined at 490 nm. In order to eliminate the scattered light of the excitation pulse, a sharp cut bandpass filter (Schott GG 475) was placed directly after the quartz lens.

Lifetime and oxygen quenching measurements were performed with a setup similar to that described above. However, the photodiode array was replaced with a photomultiplier tube (RCA IP28) and the decay signal was recorded by a 200-MHz transient digitizer (LeCroy Model TR8828). Typically, an average of 16 shots was taken for the decay signal unless specified otherwise. A 1.0-kΩ resistor was terminated on the digitizer in order to increase the intensity of the signal. This gives a RC time constant of 30 ns, which is still much faster than the decay of the emission. Thus, no further deconvolution of the decay is required. Both data acquisition and analyses were carried out by an IBM AT computer using ASYST software (ASYST Technology, Inc.).

Results and Discussion

Since the 4f orbitals are very effectively shielded from the influence of external forces by the overlying $5s^2$ and $5p^6$ shells, the states arising from the various $4f^n$ configurations are only affected by the direct coordination environment, and the second coordination sphere appears to be a negligibly small perturbation. This statement implies that if the BH---Tb(III) bonding interactions in $[H_2B(pz)_2]_3Tb$ are negligibly small, then Tb(III) sees its environment as a trigonal-prismatic configuration (D_{3h}). However, this high D_{3h} symmetry configuration will be distorted if the BH---Tb(III) bonding is strong enough to influence the 4f orbitals. Under the circumstance that the three agostically bonded hydrogen atoms are exactly in the central horizontal plane, the 4f orbital in $[H_2B(pz)_2]_3Tb$ may see C_{3h} symmetry. If this is not the case (in the solid-state structure of **1**, the yttrium atom is 0.028 Å out of the plane formed by the three boron atoms[1a]), then a lower C_3 symmetry is expected. Theoretically, these different effective point groups will change the luminescence spectral properties significantly. For a D_{3h} configuration the nine degenerate levels of $^5D_4$ in the Tb(III) ion are expected to split into six sublevels, A′, 2E′, A_1'', A_2'', and E″, by the crystal field, while the $^5D_4$ state in the C_{3h} symmetry will be split into six sublevels, A′, 2E′, 2A″, and E″. In the lower symmetry point group C_3, the crystal field splits the $^5D_4$ state into six different sublevels, 3A and 3E. This different splitting also applies to each J level in the ^7F_J ground state. The overall sublevels due to the C_{3h} or C_3 crystal field splitting are shown in Table I. The crystal splitting due to D_{3h} and D_3 are given in ref 8. Table I also shows the predicted allowed transitions from the electric dipole selection rules for each sublevel from $^5D_4 \rightarrow {}^7F_J$.

As observed from other Tb(III) complexes,[6-8] 355-nm excitation of a crystalline sample of $[H_2B(pz)_2]_3Tb$ results in strong luminescence. Seven emission groups throughout 480–700 nm can be classified. Since the luminescence analyses are based on the assignment of the number of peaks in a specific group, in order to avoid complications, determining that the spectra result solely from $^5D_4 \rightarrow {}^7F_J$ transitions is crucial. This issued has been studied in detail by the following analyses.

1. The lifetime for each individual emission group is identical with a single exponential decay rate constant of 9.17×10^2 s^{-1} (a lifetime of 1.09 ms) in the crystalline form at room temperature. When the digitizer is terminated with a 100-Ω resistor, the rise

(2) (a) Cotton, F. A.; Jeremic, M.; Shaver, A. *Inorg. Chim. Acta* **1972**, *6*, 543. (b) Kosky, C. A.; Ganis, P.; Avitable, G. *Acta Crystallogr., Sect. B: Struct. Crystallogr., Cryst. Chem.* **1971**, *B27*, 1859.
(3) Albers, M. O.; Crosby, S. F. A.; Lilies, D. C.; Robinson, D. J.; Shaver, A.; Singleton, E. *Organometallics* **1987**, *6*, 2014.
(4) (a) Reger, D. L.; Swift, C. A.; Lebioda, L. *J. Am. Chem. Soc.* **1983**, *105*, 5343. (b) Reger, D. L.; Mahtab, R.; Baxter, J. C.; Lebioda, L. *Inorg. Chem.* **1986**, *25*, 2046.
(5) *Handbook of Chemistry and Physics*; Weast, R. C., Ed.; CRC: Cleveland, OH, 1965; p F117.
(6) Brittain, H. G.; Meadows, J. H.; Evans, W. J. *Organometallics* **1983**, *2*, 1661.
(7) Brittain, H. G.; Meadows, J. H.; Evans, W. J. *Organometallics* **1985**, *4*, 1585.
(8) Brittain, H. G.; Wayda, A. L.; Mukerji, I. *Inorg. Chem.* **1987**, *26*, 2742.

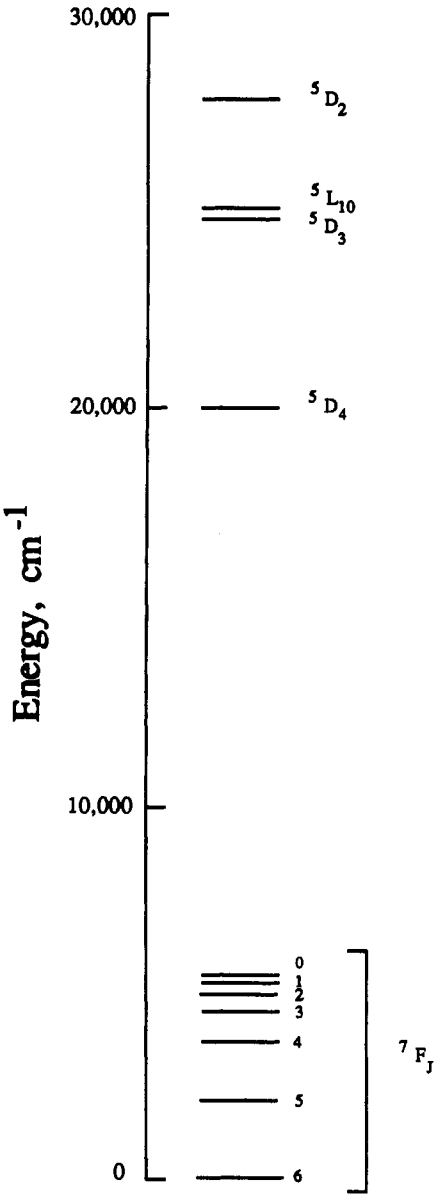

Figure 1. Energy levels for the Tb(III) ion.

time of the first five emission groups (the emission intensities for the other two are too weak to obtain a useful result) is faster than the system response time ($<1.0 \times 10^{-8}$ s). In addition, for the three higher energy groups, the spectra obtained by gating the diode array at 0–1 μs are identical with 1.0 μ–1.0 ms.

2. Using a 482-nm pulse from the dye laser leads to direct excitation of the $^7F_6 \rightarrow {}^5D_4$ transition band with no thermal population of the $^5D_3$ state at <77 K. In this case, spectra identical with those from 355-nm excitation were observed for the three higher energy emission groups (it is difficult to obtain the rest of the emission groups due to the low $^7F_6 \rightarrow {}^5D_4$ transition moment and the low energy of the dye laser ($\sim$1.0 mJ).

3. The vibronic side bands, which have frequently been observed due to the metal–ligand vibronic interaction, may interfere with the analysis of the number of the group peaks. This is particularly crucial in the range of the 4-2 ($^5D_4 \rightarrow {}^7F_2$) to 4-0 ($^5D_4 \rightarrow {}^7F_0$) transitions (hereafter we will label the $^5D_4 \rightarrow {}^7F_J$ transition levels only by their J quantum numbers), where the emission is ca. 3 orders of magnitude less than that of 4-6 due to the decrease of the spin–orbit coupling from $^7F_6$ to $^7F_0$. However, among these seven emission groups no vibrational progression can be resolved. The results of parts 1–3 clearly indicate that no emission other than from the pure f–f $^5D_4 \rightarrow {}^7F_J$ transitions is observed.

It is noted that the nine degenerate sublevels of $^5D_4$ are split into several nondegenerate states by the coordination environment and the population of each sublevel at various temperatures depends on the thermal Boltzman distribution. Thus, it is not

Table I

Selection rules governing the $^5D_4 \leftarrow {}^7F_J$ Tb(III) luminescent transitions in C_{3h} symmetry.

transition	GS	ES = A'	ES = 2E'	ES = 2A''	ES = E''	No. of bands
4-0	A'	-	++	++	-	4
4-1	A'	-	++	++	-	9
	E''	-	++	++	+	
4-2	A'	-	++	++	-	13
	E'	+	++	-	+	
	E''	-	++	++	+	
4-3	A'	-	++	++	-	17
	E'	+	++	-	+	
	2A''	++	-	-	++	
	E''	-	++	++	+	
4-4	A'	-	++	++	-	21
	2E'	++	++++	-	++	
	2A''	++	-	-	++	
	E''	-	++	++	+	
4-5	2A'	-	++++	++++	-	28
	2E'	++	++++	-	++	
	A''	+	-	-	+	
	2E''	-	++++	++++	++	
4-6	3A'	-	++++++	++++++	-	34
	2E'	++	++++	-	++	
	2A''	++	-	-	++	
	2E''	-	++++	++++	++	

Selection rules governing the $^5D_4 \leftarrow {}^7F_J$ Tb(III) luminescent transitions in C_3 symmetry.

transition	GS	ES = 3A	ES = 3E	No. of bands
4-0	A	+++	+++	6
4-1	A	+++	+++	12
	E	+++	+++	
4-2	A	+++	+++	18
	2E	++++++	++++++	
4-3	3A	+++++++++	+++++++++	30
	2E	++++++	++++++	
4-4	3A	+++++++++	+++++++++	36
	3E	+++++++++	+++++++++	
4-5	3A	+++++++++	+++++++++	42
	4E	++++++++++++	++++++++++++	
4-6	5A	+++++++++++++	+++++++++++++	54
	4E	++++++++++++	++++++++++++	

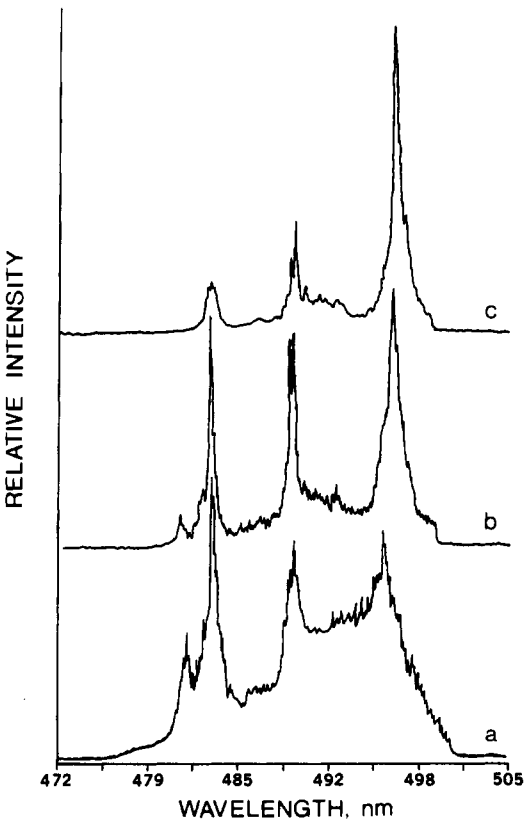

Figure 2. $^5D_4 \rightarrow {}^7F_6$ luminescence spectra of $[H_2B(pz)_2]_3Tb$ in the crystalline form at various temperatures: (a) 298 K; (b) 77 K; (c) 19 K.

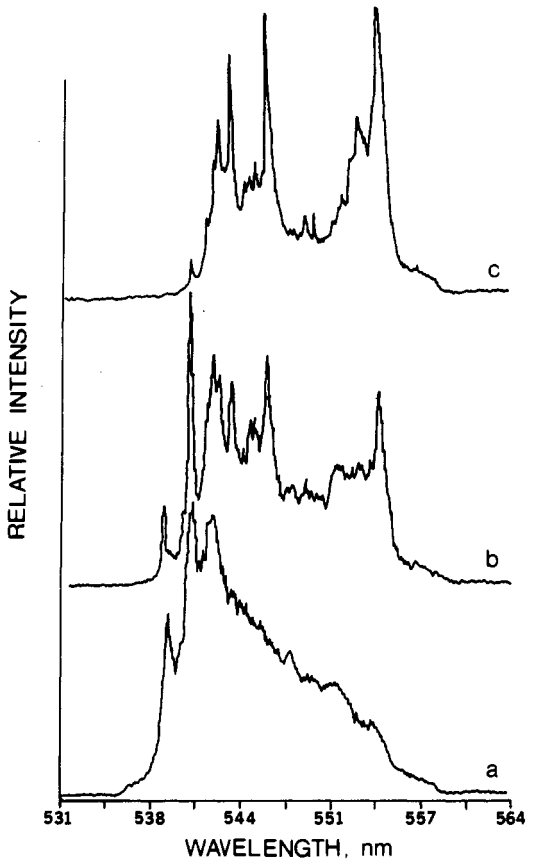

Figure 3. $^5D_4 \rightarrow {}^7F_5$ luminescence spectra of $[H_2B(pz)_2]_3Tb$ in the crystalline form at various temperatures: (a) 298 K; (b) 77 K; (c) 19 K.

necessary to analyze the luminescence spectra at extremely low temperature. This can be demonstrated in the temperature-dependent studies. Figures 2–5 select the first three emission groups 4-6, 4-5, and 4-4 as well as the last one 4-0 at various temperatures for discussion. The temperature-dependent study obviously indicates that several emission bands in the blue (higher energy) region in each emission group gradually decrease while the intensities of the emission bands in the red (lower energy) region significantly increase when the temperature decreases from 298 to 77 K. Upon further cooling to a temperature <19 K several emission peaks in each group observed at room temperature disappear, indicating that some higher energy sublevels of the $^5D_4$ state are populated negligibly at this temperature. Hence, although better spectral resolution may be obtained, the total number of allowed transitions cannot be definitively resolved at <19 K. Fortunately, our temperature-dependent studies show that even though the relative intensity of each band varied, the higher energy bands in each emission group did not vanish from 298 to 77 K, indicating that all sublevels in the $^5D_4$ state responsible for the allowed transitions are still thermally populated at 77 K. This result implies that the energy splitting between highest and lowest $^5D_4$ sublevels is small, possibly less than a few hundred reciprocal centimeters (vide infra).

Now, a crucial question to be resolved concerns how the coordination environment in the crystalline form of **2** correlates with the luminescence spectra. Assuming that all crystal field split sublevels of the $^5D_4$ state are populated at room temperature, the number of allowed transitions will be 30, 46, 34, and 54 in the case of the 4-6 transition for the symmetry point groups D_{3h}, D_3, C_{3h}, and C_3, respectively (see Table I). Since the energy difference between each sublevel transition is predicted to be small, the transition bands of the various sublevels will be obscured due to the large degree of spectral overlap in combination with the spectral inhomogeneous broadening. Thus, a thorough analysis for each group of emissions is not possible. A straightforward method that avoids complicated analysis is to analyze the 4-0

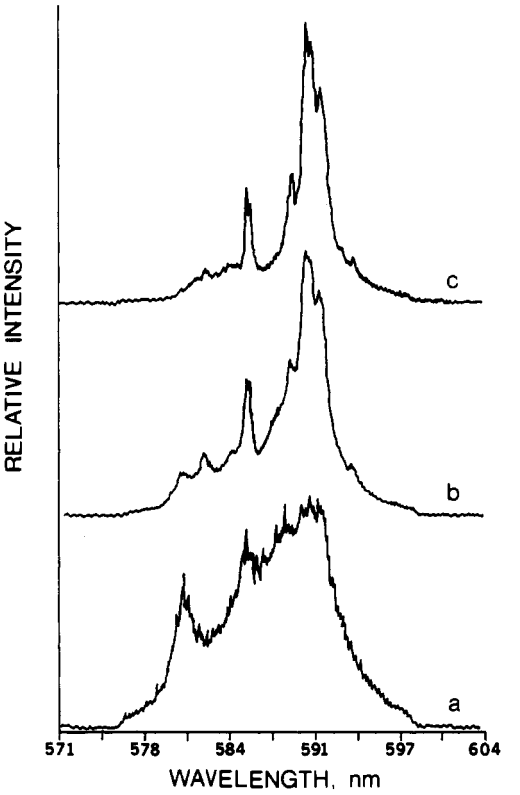

Figure 4. $^5D_4 \rightarrow {}^7F_4$ luminescence spectra of $[H_2B(pz)_2]_3Tb$ in the crystalline form at various temperatures: (a) 298 K; (b) 77 K; (c) 19 K.

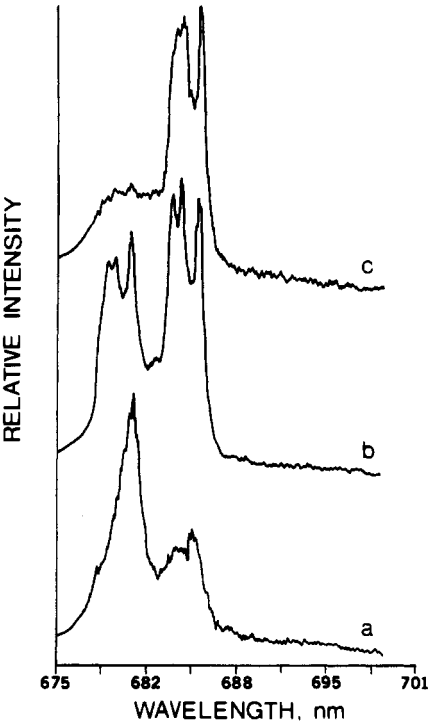

Figure 5. $^5D_4 \rightarrow {}^7F_0$ luminescence spectra of $[H_2B(pz)_2]_3Tb$ in the crystalline form at various temperatures: (a) 298 K; (b) 77 K; (c) 19 K.

transition because there is no further crystal field splitting for the $^7F_0$ state. Thus, if all six sublevels of the $^5D_4$ state can be thermally populated, the total numbers of allowed electric dipole transitions are predicted to be three, four, four, and six for D_{3h}, D_3, C_{3h}, and C_3, respectively (see Table I). Figure 5a shows the 4-0 transition located in the 675–688-nm region at 298 K. At this temperature, the broad emission spectrum makes the analysis of the number

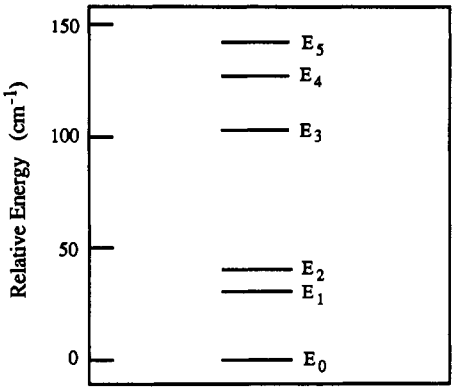

Figure 6. Relative energy for the crystal field split $^5D_4$ state in $[H_2B(pz)_2]_3Tb$.

of transition peaks impossible. Upon cooling, the emission bands in the blue region gradually decrease. In contrast, the intensities of the lower energy bands increase. Figure 5b clearly shows that the 4-0 transition consists of six peaks at 77 K. Since the corresponding ground-state $^7F_0$ has no crystal field splitting, the six emission bands originate from six crystal field split sublevels in the $^5D_4$ state. Comparing this result with the electric dipole selection rules derived in Table I for the four different symmetry point groups reveals that the coordination environment which the 4f orbitals in $[H_2B(pz)_2]_3Tb$ actually "see" is the C_3 symmetry. Thus, the luminescence spectrum is influenced by the three three-center, bridging BH---Tb agostic bonds distorting the trigonal-prismatic geometry of the nitrogen donor atoms to a lower C_3 symmetry. We note that the nonplanar chelate rings alone lowers the symmetry of the molecule to at least C_{3v}. However, it has been shown that the luminescence spectra of Tb(III) complexes are determined by the ligand arrangement of the primary coordination sphere.[6-8] Thus, the luminescence spectra would not be sensitive to this lower symmetry unless there were direct interactions such as the three-center bonds with the terbium atom.

Upon cooling of the sample to 19 K, the three peaks on the higher energy side nearly disappear (Figure 5c). The structureless hump appearing in the high-energy region at 19 K may be due to phonon interaction in the solid state. On the basis of the emission frequency at each peak maximum at 77 K, the relative energy diagram of each sublevel is depicted in Figure 6. Due to the lack of detailed information on the polarization property of each emission band, the absolute symmetry assignment for each energy level is not possible. Therefore, we label each sublevel of $^5D_4$ from E_0 to E_5 on the basis of increasing energy. The relative energy gap between the highest and lowest sublevels in $^5D_4$ is calculated to be ca. 144 cm^{-1}. Assuming that these two levels have an equal number of degenerate states for simplicity, calculation from the statistic Boltzman population gives a population ratio of 1.8×10^{-5} for E_5 with respect to E_0 at 19 K. Further calculations give population ratios of 5.61×10^{-5} and 3.48×10^{-4} for E_4 and E_3 relative to E_0, resulting in negligible emission intensity. On the other hand, population ratios of E_2 to E_0 and E_1 to E_0 are calculated to be 0.05 and 0.11, respectively. Thus, the emissions originating from E_0, E_1, and E_2 are theoretically measurable at 19 K. At 77 K, appreciable population of all six sublevels is predicted, consistent with the experimental results.

The spectral features and the lifetime of the luminescence of $[H_2B(pz)_2]_3Tb$ obtained in CH_2Cl_2 are nearly identical with those obtained in the crystalline form except that the ratio of the intensities between various peaks is slightly different. This result implies that perturbation of the coordination environment of the Tb(III) ion in CH_2Cl_2 solution versus the solid phase is negligible. Thus, we conclude that the BH---Tb agostic bonds remain intact in CH_2Cl_2 solution, consistent with the NMR results of $[H_2B(pz)_2]_3Y$ in CD_2Cl_2 solution.[1a] On the other hand, spectral broadening and change of the relative peak intensity in each group emission were observed in donor solvent such as in THF. This effect can be readily distinguished in Figure 7a,b, where the emission is taken from the 4-5 transition in THF solvent and the

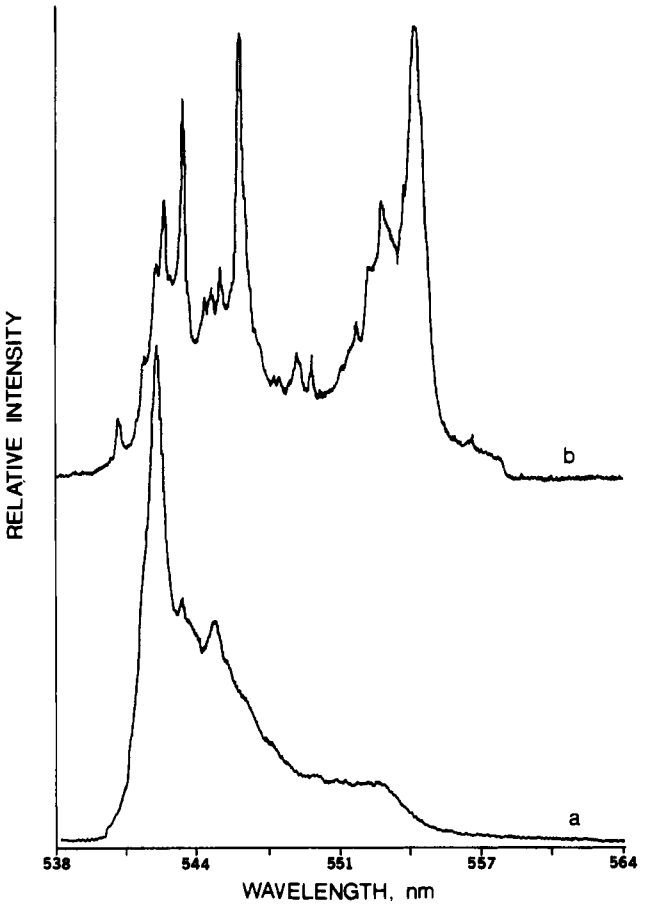

Figure 7. $^5D_4 \rightarrow {}^7F_5$ luminescence spectra of $[H_2B(pz)_2]_3Tb$ at 19 K: (a) in THF; (b) in the crystalline form.

Table II. Dynamics of the $^5D_4 \rightarrow {}^7F_J$ Luminescence in Various Solvents and Temperatures[a]

	lifetime, ms			
solvent	298 K	120 K	77 K	19 K
crystalline	1.09	1.20	1.26	1.25
toluene	1.17	1.20	1.25	1.26
CH_2Cl_2	1.17	1.20	1.25	1.26
THF	1.30	1.28	1.30	1.30
CH_3CN	1.72	1.72	1.73	1.75

[a] The error in the lifetimes is ±5%.

solid, respectively (low solubility of $[H_2B(pz)_2]_3Tb$ prevents the spectral analysis in saturated hydrocarbon solvents). However, the perturbation of the coordination environment by THF is weak due to the slight frequency shift for each emission group and the similar decay dynamics (see Table II) in comparison to that in the crystalline form. The agostic bonding may play a role in reducing the donor solvent effect. However, a quantitative conclusion for this issue cannot be made at the present stage. Table II also showed that the lifetime of the luminescence of $[H_2B(pz)_2]_3Tb$ is nearly temperature independent from 298 to 19 K in various solvents. This result is expected, since the degree of coupling between 4f orbital wavefunctions and other internal molecular motion such as various small frequency, large amplitude vibrational motions of the ligand are negligible. Similar results were observed in CH_3CN, in which the spectral feature is broader and the lifetime is significantly longer in comparison with that obtained in THF. A correlation of solvent donor ability with the lifetime has been noted previously.[8] Thus, CH_3CN is a better donor solvent for **2** than THF.

Conclusion

The spectra and dynamics of the $^5D_4 \rightarrow {}^7F_J$ luminescence of $[H_2B(pz)_2]_3Tb$ have been studied. Analysis of the spectrum of the crystalline sample based on the electron dipole selection rules

reveals an effective C_3 point group about terbium rather than D_{3h}, D_3, or C_{3h} symmetry. The spectra do not appreciably change in CH_2Cl_2 and toluene solvents. An interpretation of these results is that, in the crystalline form and in solutions of noncoordinating solvents, the three three-center, bridging BH---Tb interactions influence the luminescence spectra of **2**. In donor solvents, complexation of $[H_2B(pz)_2]_3Tb$ with the solvent molecules changes the lifetime and the spectral features of the luminescence. For these cases, coordination of the solvent results in a change in the coordination environment about terbium.

Contribution from the Department of Chemistry,
York University, North York (Toronto), Ontario, Canada M3J 1P3

Control of Orbital Mixing in Ruthenium Complexes Containing Quinone-Related Ligands

Hitoshi Masui, A. B. P. Lever,* and Pamela R. Auburn

Received August 14, 1990

Three redox series of complexes of the general formulas $Ru^{II}(bpy)_2LL$ and $Ru^{II}(py)_4LL$ (bpy = 2,2'-bipyridine) are reported, where LL are the ligands 1,2-dihydroxybenzene, 2-aminophenol, and 1,2-diaminobenzene. These ligands can exist in the fully reduced catechol form or the one and two electron oxidized semiquinone and quinone forms. Electronic and electron spin resonance spectroscopic and electrochemical data are discussed in terms of orbital mixing and electronic structure and the number of oxygen or nitrogen atoms in the coordinating ligand.

Introduction

There has been considerable interest in the study of transition-metal complexes of noninnocent, quinone-related ligands including those of dithiolenes,[1-3] dioxolenes,[4-16] and benzoquinonediimines.[17-33] The possibility of electron delocalization between the metal and the ligand has been a major theme in the study of these systems.[30,34-36] The electron distribution will depend on the extent of mixing between the metal and ligand orbitals, which, in turn, is a function of the energies, symmetries, and overlap of the valence metal and ligand orbitals.

Previous studies of ruthenium dioxolene complexes (dioxolene = catechol, semiquinone, quinone)[7-9] have found unusually large

Scheme I. *o*-Phenylene Ligand Redox Isomers[a]

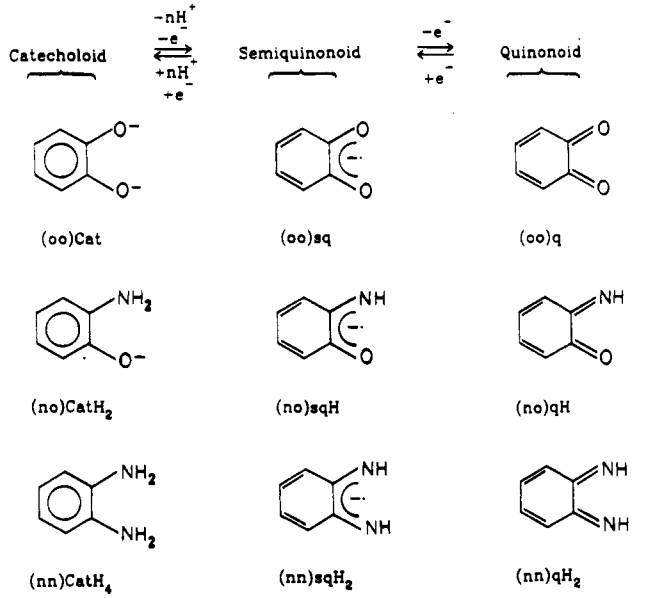

[a] Key: for (nn), $n = 2$; for (no), $n = 1$; for (oo), $n = 0$.

(1) Burns, R. P.; McAuliffe, C. A. *Adv. Inorg. Chem. Radiochem.* **1979**, *22*, 303.
(2) Eisenberg, R. *Prog. Inorg. Chem.* **1970**, *12*, 295.
(3) McCleverty, J. A. *Prog. Inorg. Chem.* **1968**, *10*, 49.
(4) Kessel, S. L.; Emerson, R. M.; Debrunner, P. G.; Hendrickson, D. N. *Inorg. Chem.* **1980**, *19*, 1170.
(5) Buchanan, R. M.; Claflin, J.; Pierpont, C. G. *Inorg. Chem.* **1983**, *22*, 2552.
(6) Harmalker, S.; Jones, S. E.; Sawyer, D. T. *Inorg. Chem.* **1983**, *22*, 2790.
(7) Haga, M.-A.; Dodsworth, E. S.; Lever, A. B. P. *Inorg. Chem.* **1986**, *25*, 447.
(8) Stufkens, D. J.; Snoeck, Th. L.; Lever, A. B. P. *Inorg. Chem.* **1988**, *27*, 935.
(9) Lever, A. B. P.; Auburn, P. R.; Dodsworth, E. S.; Haga, M.-A.; Liu, W.; Melnik, M.; Nevin, W. A. *J. Am. Chem. Soc.* **1988**, *110*, 8076.
(10) Thompson, J. S.; Calabrese, J. C. *Inorg. Chem.* **1985**, *24*, 3167.
(11) Sofen, S. R.; Ware, D. C.; Cooper, S. R.; Raymond, K. N. *Inorg. Chem.* **1979**, *18*, 234.
(12) Boone, S. R.; Pierpont, C. G. *Inorg. Chem.* **1987**, *26*, 1769.
(13) Espinet, P.; Bailey, P. M.; Maitlis, P. M. *J. Chem. Soc., Dalton Trans.* **1979**, 1542.
(14) Pierpont, C. G.; Buchanan, R. M. *Coord. Chem. Rev.* **1981**, *38*, 45.
(15) Cooper, S. R.; Koh, Y. B.; Raymond, K. N. *J. Am. Chem. Soc.* **1982**, *102*, 5092.
(16) Benelli, C.; Dei, A.; Gatteschi, D.; Pardi, L. *Inorg. Chem.* **1989**, *28*, 1476.
(17) Balch, A. L.; Holm, R. H. *J. Am. Chem. Soc.* **1966**, *88*, 5201.
(18) Baikie, P. E.; Mills, O. S. *Inorg. Chim. Acta* **1967**, *1*, 55.
(19) Duff, E. J. *J. Chem. Soc. A* **1968**, 434.
(20) Warren, L. F. *Inorg. Chem.* **1977**, *16*, 2814.
(21) Reinhold, J.; Benedix, R.; Birner, P.; Hennig, H. *Inorg. Chim. Acta* **1979**, *33*, 209.
(22) Vogler, A.; Kunkely, H. *Angew. Chem., Int. Ed. Engl.* **1980**, *19*, 221.
(23) Belser, P.; von Zelewsky, A.; Zehnder, M. *Inorg. Chem.* **1981**, *20*, 3098.
(24) El'Cov, A. V.; Maslennikova, T. A.; Kukuschkin, V. Ju.; Shavurov, V. V. *J. Prakt. Chem.* **1983**, *B325*, S27.
(25) Pyle, A. M.; Barton, J. K. *Inorg. Chem.* **1987**, *26*, 3820.
(26) Thorn, D. L.; Hoffmann, R. *Nouv. J. Chim.* **1979**, *3*, 39.
(27) Peng, S.-M.; Chen, C.-T.; Liaw, D.-S.; Chen, C.-I.; Wang, Y. *Inorg. Chim. Acta* **1985**, *101*, L31.
(28) Christoph, G. G.; Goedken, V. L. *J. Am. Chem. Soc.* **1973**, *95*, 3869.
(29) Hall, G. S.; Soderberg, R. H. *Inorg. Chem.* **1968**, *7*, 2300.
(30) Gross, M. E.; Ibers, J. A.; Trogler, W. C. *Organometallics* **1982**, *1*, 530.
(31) Zehnder, M.; Loliger, H. *Helv. Chim. Acta* **1980**, *63*, 754.
(32) Danopoulos, A. A.; Wong, A. C. C.; Wilkinson, G.; Hursthouse, M. B.; Hussain, B. *J. Chem. Soc., Dalton Trans.* **1990**, 315.
(33) Nemeth, S.; Simandi, L. I.; Argay, G.; Kalaman, A. *Inorg. Chim. Acta* **1989**, *166*.
(34) Gross, M. E.; Trogler, W. C.; Ibers, J. A. *J. Am. Chem. Soc.* **1981**, *103*, 192.
(35) Miller, E. J.; Brill, T. B. *Inorg. Chem.* **1983**, *22*, 2392.
(36) Miller, E. J.; Landon, S. J.; Brill, T. B. *Organometallics* **1985**, *4*, 533.

0020-1669/91/1330-2402$02.50/0